Journal of Geochemical Exploration 238 (2022) 107004

Contents lists available at ScienceDirect

Journal of Geochemical Exploration

journal homepage: www.elsevier.com/locate/gexplo

In situ U-Pb dating of calcite indicates a Miocene Sb-Pb mineralization event in the Sanjiang base metal metallogenic belt, SW China

Xiangyuan Sheng[a,b], Yongyong Tang[b,*], Xianwu Bi[b], Ruizhong Hu[b], Leiluo Xu[b], Juan Li[b,c], Yanwen Tang[b]

[a] College of Resources and Environmental Engineering, Mianyang Normal University, Mianyang 621000, Sichuan, China
[b] State Key Laboratory of Ore Deposit Geochemistry, Institute of Geochemistry, Chinese Academy of Sciences, Guiyang 550081, China
[c] University of Chinese Academy of Sciences, Beijing 100049, China

A R T I C L E I N F O

Keywords:
In situ U-Pb dating
Zn-Pb-Sb deposit
Lanuoma
Sanjiang base metal metallogenic belt (SMB)

A B S T R A C T

The Sanjiang base metal metallogenic belt (SMB) in southwestern China is characteristic of composite mineralization during the India-Asia continental collision. However, the geodynamic settings of the composite processes of this belt are poorly understood. The Lanuoma deposit, located in the Changdu Basin in the central segment of the SMB, is a Zn-Pb-Sb polymetallic deposit. The cross-cutting relationships and paragenetic mineral associations suggest the superimposition of a late Sb-Pb mineralization event over an early Zn-dominant mineralization event. Calcite is the main gangue mineral, intergrown with late Sb-Pb minerals (e.g., boulangerite, zinkenite, sorbyite and plagionite). In situ U-Pb dating by laser ablation-inductively coupled plasma mass spectrometry (LA-ICPMS) was successfully carried out on calcite from this deposit, and restricts the Sb-Pb mineralization to 19.7 ± 1.6 Ma, with a mean square weighted deviation (MSWD) of 1.2. This age is approximately synchronous with that of strike-slip shearing-related leucogranites in the marginal orogens; together with previous data, this result suggests that the contemporaneous magmatism significantly contributed to the ore-forming fluids associated with the Sb-Pb mineralization. Overprinting of the Miocene Sb-Pb event in a transtensional regime on the Oligocene transpression-driven Zn mineralization resulted in the characteristic Zn-Pb-Sb assemblage at Lanuoma. Moreover, this study indicates that the SMB holds great exploration potential for Sb(-Pb) resources.

1. Introduction

The Sanjiang base metal metallogenic belt (SMB; Fig. 1) is one of the most important producers of base metals (e.g., Pb, Zn, Cu, Sb and Co) in China (Hou et al., 2008; Liu et al., 2017b; Song et al., 2017; Bi et al., 2019; Leach and Song, 2019). This belt contains several economically significant large to giant Pb-Zn polymetallic deposits (e.g., Huoshaoyun, Jinding, Baiyangping, Mohailaheng and Chaqupacha) and numerous small-medium deposits, which are mainly distributed in the Tianshuihai, Tuotuohe, Yushu, Changdu and Lanping areas. The deposits are hosted in Mesozoic limestones and sandstones and are spatially controlled by Cenozoic fault systems associated with the India-Asia continental collision (Hou et al., 2008; He et al., 2009; Hou and Zhang, 2015). Although many studies have considered the SMB to be a Mississippi Valley-type (MVT) belt (Leach et al., 2017; Song et al., 2017; Leach and Song, 2019), characteristic polymetallic assemblages (e.g., Pb-Zn-(Ag-Cu-Co, Sb-Hg and Cd-Tl)) distinguish it from the typical polymetallic assemblages (e.g., Pb-Zn-(Ag) of MVT deposits). Most recent studies have suggested that the composite mineralization of basinal brine, meteoric water and magmatic fluid can be used to interpret the SMB (Tao et al., 2011; Wang et al., 2011b; Deng et al., 2014; Bi et al., 2019). However, the detailed geodynamic settings and processes remain poorly constrained.

Geochronological advances show a peak of 38–28 Ma for the Pb-Zn mineralization in the SMB (Wang et al., 2011a; Zou et al., 2015; Liu et al., 2016; Feng et al., 2017; Yalikun et al., 2018; Bi et al., 2019; Zhang et al., 2019), corresponding to the late-collisional stage of tectonic transformation (from compression to extension) of the India-Asia collision (Hou and Cook, 2009). Because of possible inclusions (e.g., carbonate and clay minerals) in sphalerite, Bradley et al. (2004) and Kesler et al. (2004) expressed their concern about the reliability of sphalerite Rb-Sr isotope isochron ages for MVT Pb-Zn deposits. As most of the

* Corresponding author.
E-mail address: tangyongyong@vip.gyig.ac.cn (Y. Tang).

https://doi.org/10.1016/j.gexplo.2022.107004
Received 18 May 2021; Received in revised form 7 April 2022; Accepted 16 April 2022
Available online 21 April 2022
0375-6742/© 2022 Elsevier B.V. All rights reserved.

sphalerite Rb-Sr isotope dates for the SMB Pb-Zn deposits are consistent (with an age cluster of 33–28 Ma) and agree with the Sm-Nd isotope dates of the intergrown calcites (Wang et al., 2011a; Zou et al., 2015; Feng et al., 2017; Bi et al., 2019), these sphalerite Rb-Sr dating data likely represent the timing of the early Pb-Zn ore formation. Very few data are available to constrain the late base metal mineralization timing for two possible reasons: 1) a lack of minerals suitable for conventional radioisotopic dating and 2) the influence by earlier ores.

The Lanuoma deposit, located in the Changdu Basin in the central SMB, has a metal assemblage of Pb-Zn-Sb. Field observations show two episodes of hydrothermal mineralization: an early Zn-dominated mineralization episode and a late Sb-Pb mineralization episode, represented by an early sphalerite-pyrite assemblage and a late Sb-Pb-sulfosalt-sphalerite-calcite-orpiment-realgar assemblage, respectively (Sheng et al., 2019). Sphalerite Rb-Sr dating produces an isochron age of 30 Ma (Bi et al., 2019), which likely represents the age of the early Zn mineralization episode. The results of this study provide a constraint on the timing of the late Sb-Pb mineralization episode based on in situ laser ablation-inductively coupled plasma mass spectrometry (LA-ICPMS) U-Pb dating of calcite, which indicates that a Miocene Sb-Pb mineralization event occurred in the transtensional setting of the India-Asia collision. Moreover, a model of fluid mixing between shallow fluid (e.g., basinal brine) and magmatic fluid is proposed for Sb-Pb mineralization of the Lanuoma deposit, which provides significant insights into the metallogenesis within the SMB.

2. Geological setting and ore deposit characteristics

The SMB, restricted between the Jinshajiang and Nujiang sutures within the North Qiangtang and Changdu-Simao blocks (Fig. 1; Pan et al., 1997; Zhong, 1998; Metcalfe, 2002), is in the eastern India-Asia collision zone along the northern to northeastern margin of the Tibetan Plateau. The belt extends over a thousand kilometres and is characterized by a series of large-scale Cenozoic thrust and strike-slip fault systems, Tertiary foreland basins and Cenozoic potassic-ultrapotassic igneous rocks (Hou et al., 2008). The Tertiary basins, developed on a Precambrian to Palaeozoic metamorphic basement (Zhai and Cong, 1993; Yin et al., 1999; Wang et al., 2000), underwent late Triassic rifting and Jurassic to Cretaceous depression (Yin and Harrison, 2000; Pan et al., 2003; Spurlin et al., 2005), filled with shallow marine clastic and carbonate rocks and marine-terrestrial to terrestrial red clastic rocks (Mu et al., 1999; Zhong et al., 2000; Liao and Chen, 2005). Associated with the crustal contraction caused by the India-Asia collision in the early Eocene (prior to 51 Ma; Spurlin et al., 2005), the Mesozoic depression basins evolved into isolated foreland basins filled with lake-facies siliciclastic rock sequences (Mu et al., 1999; Spurlin et al., 2005). These basins underwent four stages of deformation in the Cenozoic: Palaeocene-Eocene compression (~65–42 Ma), Eocene-Oligocene transpression (~40–26 Ma), early mid-Miocene transtension (~25–18 Ma) and late Neocene extension (<18 Ma; Wang et al., 2001; Hou et al., 2006). The south-north-trending and/or northwest-southeast-trending thrust faults defined the major tectonic framework of the SMB and remained episodically active because of the crustal shortening caused by the India-Asia collision during the Eocene (50–37 Ma; Hou et al., 2006). These thrusts were overprinted by strike-slip faults that initially occurred at 42 Ma and lasted to 23 Ma with early-stage sinistral and late-stage dextral movements (Tapponnier et al., 1990; Hou et al., 2003; Spurlin et al., 2005; Liu et al., 2006).

Cenozoic magmatism in the Sanjiang region clustered into three episodes: Palaeocene to early Eocene, middle Eocene to late Oligocene

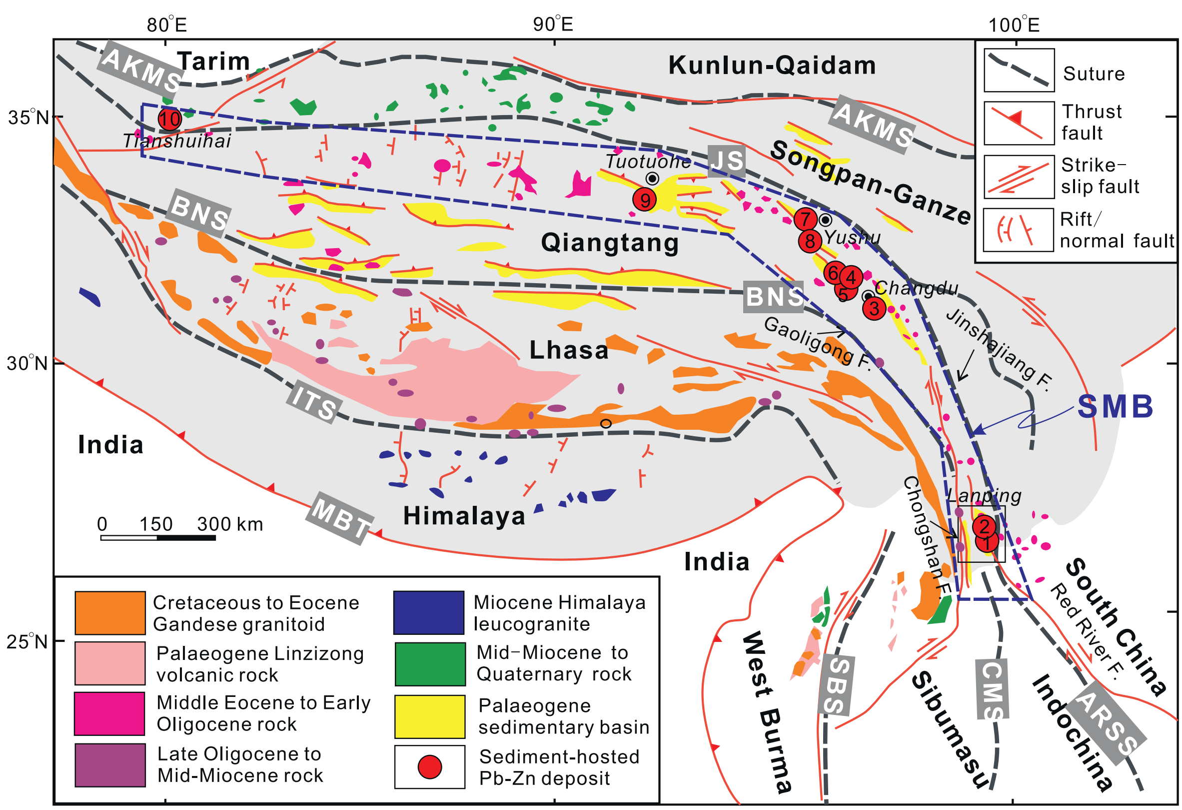

Fig. 1. Simplified geological map showing the location of the SMB along the northern to northeastern margin of the Tibetan Plateau (modified from Chung et al., 2005; Wang et al., 2010). The numbers in the solid red circles indicate major Pb-Zn deposits: 1, Jinding; 2, Baiyangping; 3, Lanuoma; 4, Zhaofayong; 5, Lalongla; 6, Jiamoshan; 7, Dongmozhazhua; 8, Mohailaheng; 9, Chaqupacha and 10, Huoshaoyun. Abbreviations: AKMS, Animaqing-Kunlun-Muztagh suture; JS, Jinshajiang suture; ARSS, Ailaoshan-Red River shear zone; BNS, Bangong-Nujiang suture; ITS, Indus-Tsangpo suture; MBT, Main Boundary thrust and CMS, Changning-Menglian suture. (For interpretation of the references to colour in this figure legend, the reader is referred to the web version of this article.)

and late Miocene to Holocene (Fig. 1). Evidence of Palaeocene to early Eocene magmatic activity is mainly distributed in the Tengchong block, with ages from 62 to 47 Ma, resulting from Neotethyan oceanic slab subduction (Xu et al., 2012; Chen et al., 2014). The middle Eocene to early Oligocene magmatism comprises the following: 1) late Eocene intraplate magmatism, expressed as mafic dykes (42–39 Ma) in the Gaoligongshan shear zone and eastern margin of the Tengchong block and generated by partial melting of metasomatized lithospheric mantle in response to asthenospheric upwelling following the breakoff of the subducted Neotethyan oceanic slab (Xu et al., 2008); and 2) middle Eocene to early Oligocene potassic-ultrapotassic igneous rocks along the Jinshajiang-Ailaoshan tectonic belt, which display increasingly younger ages from the northern segment (41–36 Ma) to the southern segment (~35 Ma) and likely formed as a magmatic expression of lower lithospheric mantle delamination (Hou et al., 2003; Lu et al., 2012; Deng et al., 2014). The late Miocene to Holocene magmatism is mainly Pleistocene-Holocene volcanic rocks in the northern and southern segments of the Sanjiang domain, which are genetically ascribed to decompression melting of the asthenosphere associated with subduction-induced metasomatism (Wang et al., 2001; Zhou et al., 2012; Flower et al., 2013).

Above the metamorphic base of the Jitang and Youxi Groups, the Changdu Basin was filled with Triassic to Palaeogene marine carbonate and terrigenous siliciclastic sedimentary rocks (Fig. 2a). Indosinian magmatism occurred as granodiorite and biotite granites in the southern basin and as rhyolites and dacites in the northern basin (Tao et al., 2014; Bi et al., 2019). Cenozoic felsic rocks (e.g., monzogranite, quartz monzonite, granite porphyry and syenite porphyry) are mainly exposed around Yulong in the northern basin and locally in the southern basin (Hou et al., 2003; Guo et al., 2006; Jiang et al., 2006). After the India-Asia continental collision, the tectonic activities of the Changdu Basin were characterized by thrust and strike-slip faults during the Eocene to Oligocene, which controlled the distribution of major ore deposits in the basin (Tang et al., 2006). Pb and Zn deposits, e.g., Jiamoshan, Zhaofayong, Lalongla, Lanuoma and Cuona, are mainly localized within the Lancangjiang thrust system, which constitutes a northwest-southeast-trending metallogenic belt across Leiwuqi and Zuogong Counties.

The Lanuoma deposit is located in the central Changdu Basin. The strata exposed in the mining area contain the Upper Triassic Jiapila, Bolila, Adula and Duogaila Formations and Quaternary sediments (Fig. 2b). The Duogaila, Adula and Jiapila Formations consist mainly of greywacke, mudstone, shales and sandstones, and the Bolila Formation consists of clastic rocks and microcrystalline limestone. The deposit consists of two orebodies (I and II) hosted by the limestone of the Bolila Formation (Fig. 2b). Orebody I is predominantly composed of Zn, whereas orebody II is predominantly composed of Sb (inferred resource: 253 hundred tons; Feng et al., 2006) and Pb. Two-stage mineralizations consisting of early Zn-dominated mineralization and late Sb-Pb mineralization exist in the Lanuoma deposit (Fig. 3a, b; Sheng et al., 2019). The primary ore minerals are mainly sphalerites, S-Sb-Pb minerals (Sb-Pb sulfosalts), pyrite, orpiment and realgar (Fig. 3c, d; Sheng et al., 2019). The Sb-Pb sulfosalts mainly consist of boulangerite, zinkenite, sorbyite and plagionite (Sheng et al., 2019). Generally, sphalerite formed earlier than the Sb-Pb minerals and coexist with minor pyrite (Fig. 3b, d, e,); the Sb-Pb minerals are mainly intergrown with calcite (Fig. 3b, e,), and minor sphalerite formed in association with Sb-Pb minerals (Fig. 3f).

3. Sample preparation and analysis methods

In situ U-Pb dating was performed on calcite intergrown with S-Sb-Pb minerals (Fig. 4). Samples were polished into thin sections before examination by optical microscopy to confirm generations. U and Pb isotope ratios were measured using an LA-ICPMS instrument equipped with an Agilent 7900 quadruple mass spectrometer and a GeoLASpRO 193 nm ArF excimer laser, at the State Key Laboratory of Ore Deposit Geochemistry, Institute of Geochemistry, Chinese Academy of Sciences. The parameters for ablation were as follows: spot size, 120 μm; repetition rate, 10 Hz; and energy density, 8 J/cm^2. The samples and standards were ablated for 3–5 pulses to clean the surfaces before formal ablation. Before entering the torch, the aerosols were carried by pure helium (450 ml/min) and mixed with argon via a T-connector. Pure nitrogen (~3.0 ml/min) was added to the helium carrier gas to increase the sensitivity via a Y junction before entering the ICP (Hu et al., 2008). The standard-sample bracketing approach was used to measure ^{202}Hg, ^{204}Pb, ^{206}Pb, ^{207}Pb, ^{208}Pb, ^{232}U and ^{238}U. Each analysis involved 20 s for background

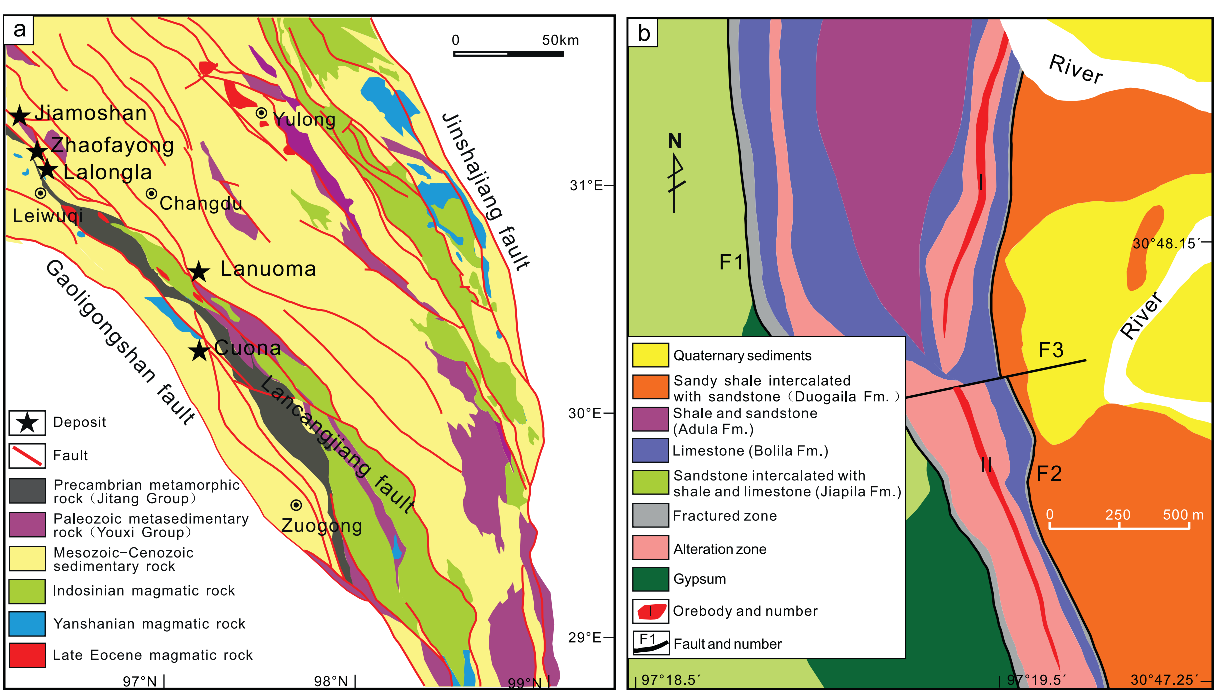

Fig. 2. Geological maps of the Changdu Basin (a; modified from Pan et al., 2004) and the Lanuoma deposit (b; modified from Feng et al., 2006).

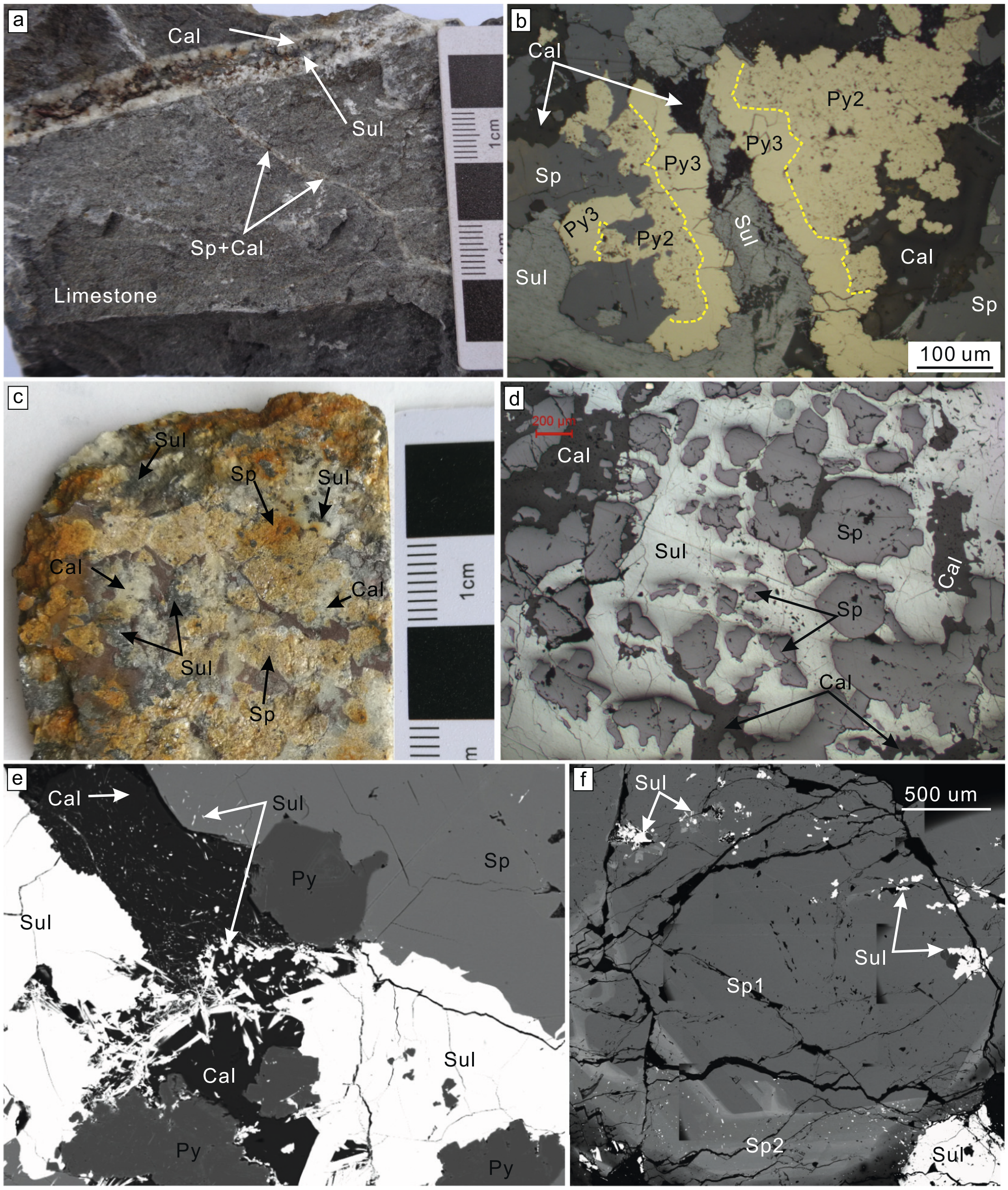

Fig. 3. Mineral association shows two mineralization stages of the Lanuoma deposit. a and b (b; modified from Sheng et al., 2019) reveal that late S-Sb-Pb minerals-calcite veins cut early sphalerite-calcite veins. The hand specimen in c shows the major primary ore minerals. d and e show that S-Sb-Pb minerals coexist with calcite but cut sphalerites. f shows that Sp1 is overgrown by Sp2, and Sp2 is associated with S-Sb-Pb minerals. Abbreviations: Py, pyrite; Sp, sphalerite; Sul, S-Sb-Pb minerals; Cal, calcite.

acquisition, 30 s for data acquisition and 40 s for the elimination of memory effects. NIST 614 was used to correct the $^{207}Pb/^{206}Pb$ ratios, and a matrix-matched carbonate reference (WC-1) was used for fractionation correction of the $^{238}U/^{206}Pb$ ratios. Data reduction was performed using the program ICPMSDataCal (Liu et al., 2008). Other details can be found in Roberts and Walker (2016) and Roberts et al. (2017).

4. Results

In total, 90 analyses of calcite associated with S-Sb-Pb minerals were conducted, which yielded Pb concentrations of 0.09 to 9.85 ppm, ^{232}Th values of 0.04 to 1.97 ppm and ^{238}U values of 0.10 to 2.58 ppm. The $^{238}U/^{206}Pb$ ratios ranged from 0.05 to 35.08, and the $^{207}Pb/^{206}Pb$ ratios ranged from 0.730 to 0.843 (Suppl. A1), revealing a lower intercept age of 19.7 ± 1.6 Ma with an initial $^{207}Pb/^{206}Pb$ value of 0.820 and a mean square weighted deviation (MSWD) of 1.2 in the Tera-Wasserburg diagram (Fig. 4).

5. Discussion

5.1. Timing of the Sb-Pb mineralization episode

The $^{207}Pb/^{206}Pb$ ratios of the S-Sb-Pb minerals range from 0.817 to 0.821, with an average value of 0.820 (our unpublished data). Because the amounts of massed radiogenic Pb are negligible in the Sb-Pb minerals due to their extremely low U contents, the $^{207}Pb/^{206}Pb$ compositions of the Sb-Pb minerals are approximately identical to those of the precipitating fluids. The initial $^{207}Pb/^{206}Pb$ value of the dated calcite approximates that of the precipitating fluid, which implies that the influence of common Pb and post-ore modification are negligible. In

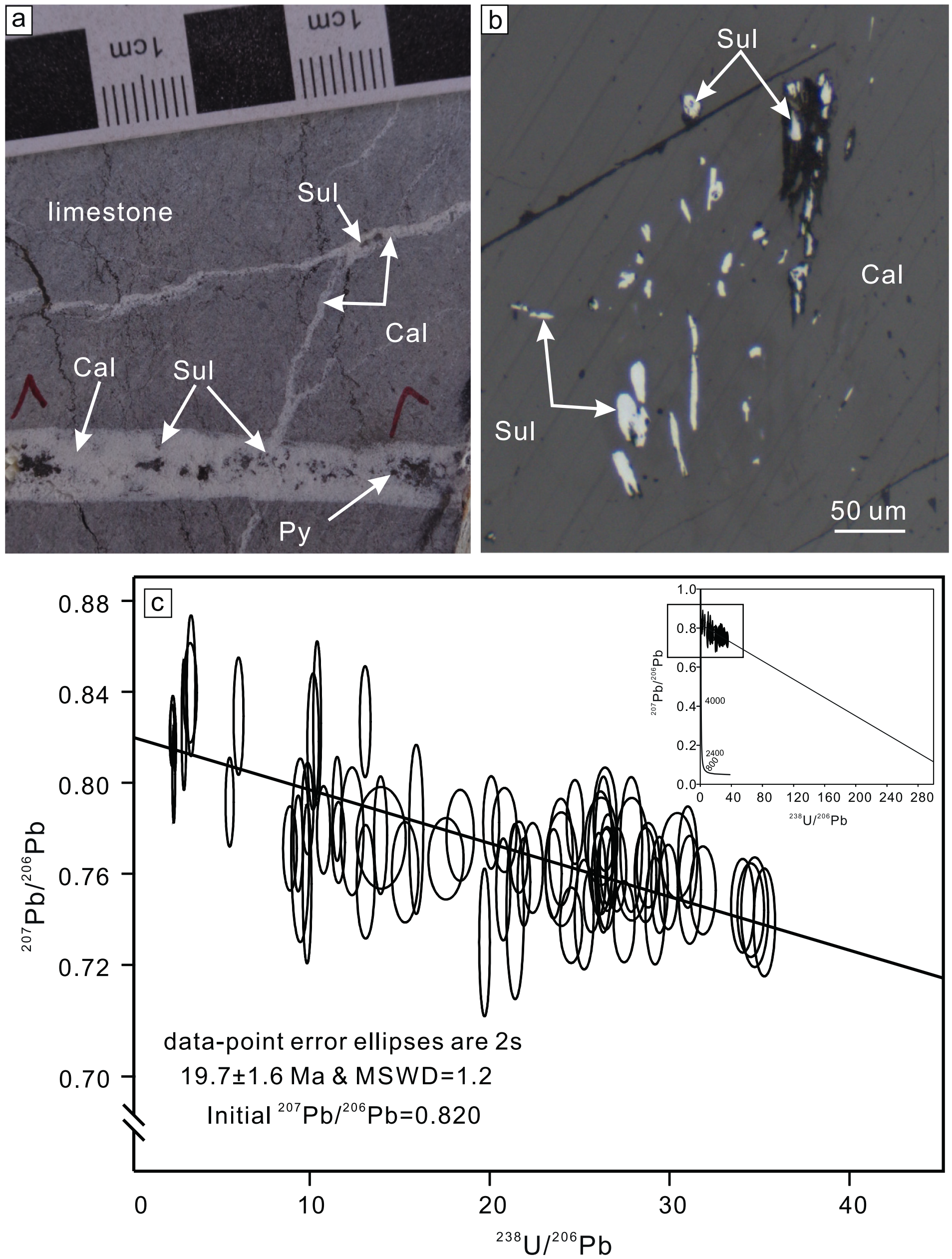

Fig. 4. In situ U-Pb dating of calcite from the Lanuoma deposit. a and b show the dated calcite, intergrown with Sb-Pb minerals; c shows the U-Pb age of calcite in the Tera-Wasserburg diagram. Data are from Suppl. A1. Abbreviations: Cal, calcite; Sul, Sb-Pb minerals; Sp, sphalerite; Py, pyrite.

addition, the Lanuoma deposit is an epithermal deposit, as indicated by the ore textures, which should have formed after the deposition of the host rocks (Bolila Formation >200 Ma) and the ore-controlling thrust faults (initially occurring in the Eocene) (Tang et al., 2006). Moreover, the paragenetic mineral associations suggest that the Lanuoma deposit consists of early Zn-dominant mineralization and late Sb-Pb mineralization (Sheng et al., 2019), and Bi et al. (2019) reported an early Zn mineralization age of 30 Ma. Thus, the calcite age agrees with these geological constraints, and the calcite U-Pb age (19.7 ± 1.6 Ma) likely represents the Sb-Pb mineralization age at Lanuoma.

5.2. Genesis of the Lanuoma deposit and regional significance

Wang et al. (2001) suggested that the interval of 24–17 Ma represents a geodynamic transition from processes controlled mainly by crustal deformation to those dominated by mantle tectonics in the evolution of the eastern India-Asia collision zone. Temporally, the age of the Lanuoma Sb-Pb mineralization agrees well with the timing of leucogranite intrusions related to ductile left-lateral shearing along three main shear zones (i.e., Chongshan, Gaoligongshan and Ailaoshan-Red River; Figs. 1 and 5) in the southern Sanjiang region (Deng et al., 2014). Studies have shown that regional sinistral strike-slip shearing was almost contemporaneously initiated ca. 32 Ma and terminated ca. 20–17 Ma (Searle et al., 2010; Cao et al., 2011; Liu et al., 2012; Tang et al., 2013); it subsequently transitioned to dextral movements (Zhang et al., 2010; Deng et al., 2014). Such a transition could have resulted in a rapid release of pressure on the planes of faults, upwelling of the underlying fluids along the faults and their discharge upon mixing with local fluids. Xu (2017) suggested that deep fluids with higher $^{3}He/^{4}He$ ratios (0.09–0.14 Ra for fluid inclusions in S-Sb-Pb minerals) contributed to the late Sb-Pb mineralization episode. Based on the $\delta^{34}S_{CDT}$ values (-1.6 to +6.0‰) of S-Sb-Pb minerals (boulangerite), orpiment and

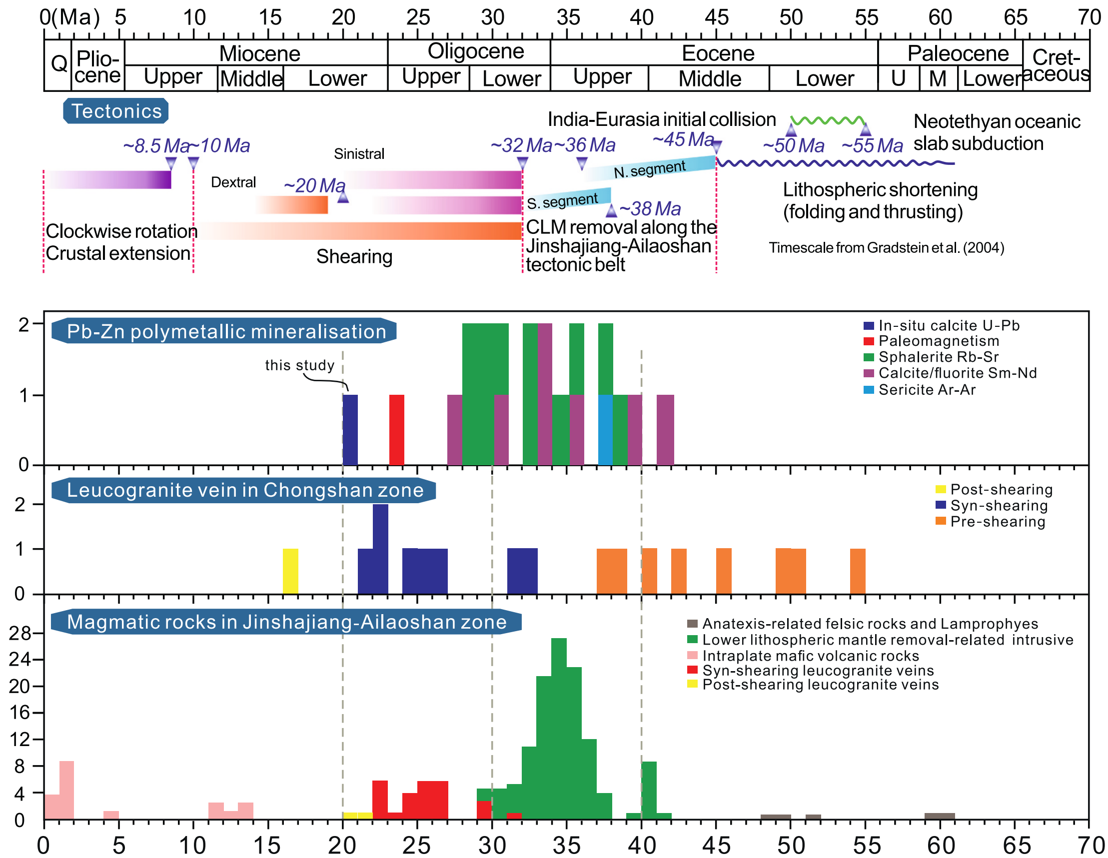

Fig. 5. Tectono-magmatic-metallogenic events in and around the SMB. The data are from Suppl. A2, Deng et al., 2014, and references therein. Abbreviations: CLM-continental lithosphere mantle.

pyrite from the late Sb-Pb mineralization episode, magmatic sulfur and sulfate-reduced sulfur (e.g., sulfur originating from gypsum via thermochemical sulfate reduction) have been suggested to have jointly participated in the Sb-Pb mineralization (Tao et al., 2011; Yang, 2011; Xu, 2017; Sheng et al., 2019). Furthermore, $\delta^{13}C_{PDB}$ (-4.7 to +0.4‰; Xu, 2017) and $\delta^{18}O_{SMOW}$ (+14.2 to +20.4‰; Xu, 2017) data of calcite from the Sb-Pb mineralization also display composite signals between the deep fluid ($\delta^{13}C_{PDB}$ of mantle: -5 to -2‰; $\delta^{13}C_{PDB}$ of magma: -9 to -3‰; Taylor, 1986) and sedimentary carbonates ($\delta^{13}C_{PDB}$: -2 to +3‰, approximately 0‰; Veizer et al., 1980). As a result, the ore-forming fluid of Sb-Pb mineralization is characterized by moderate-low homogenization temperatures (208–297 °C) and a wide range of salinities (3.2–17.1 wt% $NaCl_{eq.}$) measured from fluid inclusions in orpiment from the late Sb-Pb mineralization (Xu, 2017). Therefore, fluid inclusions and S, C-O and He isotope data suggest the participation of magmatic components in the Sb-Pb mineralization of the Lanuoma deposit (Tao et al., 2011; Xu, 2017; Sheng et al., 2019), which implies that the magmatic components were most likely sourced from contemporaneous magmatism related to strike-slip shearing and resulting from the remelting of crustal materials (Wang et al., 2006; Zhang et al., 2010; Liu et al., 2015). Some analogues may refer to the Zhaxikang, Rujevac and Čumavići Pb-Zn-Sb deposits in the Tethyan domain, which have been shown to share a genetic relationship with coeval felsic magmatism (Janković et al., 1977; Radosavljević et al., 2014, 2016; Xie et al., 2017; Zhou et al., 2018; Wang et al., 2019). It is postulated that the ~20 Ma magmatic fluid induced by coeval shearing strike-slip movements along the margins of the Cenozoic basins was transported along the detachment zone of large-scale thrust systems and then mingled with shallow fluid (e.g., basinal fluid); metals subsequently precipitated due to fluid mixing and/or cooling (e.g., at Lanuoma) during the transition from transpression to transtension (Fig. 6a).

Bi et al. (2019) reported an isochron age of 30 Ma using sphalerite Rb-Sr dating at Lanuoma, consistent with the ages (28–38 Ma) of most Pb-Zn deposits in the SMB (Fig. 5), likely reflecting a regional prolonged hydrothermal Pb-Zn event. Many studies have considered that this episode of Pb-Zn mineralization was closely associated with the circulation of basinal brines (Liu et al., 2017b; Tang et al., 2017; Wang et al., 2017; Bi et al., 2019; Mu et al., 2021). Notably, the 38–28 Ma Pb-Zn deposits display synchronization with the potassic-ultrapotassic igneous rocks (~40–26 Ma; Deng et al., 2014) along the Jinshajiang-Ailaoshan tectonic belt. In particular, the Pb-Zn deposits in the northern segment of the SMB appear slightly older than those in the southern SMB. For example, calcite Sm-Nd dating shows ages of 41–38 Ma for the Jiamoshan, Zhaofayong and Lalongla deposits in the Changdu Basin (Liu et al., 2016), in contrast to the ages of the deposits (approximately 30 Ma or younger) within the Lanping Basin; these differences are likely related to the distinct tectonic locations of these deposits (Deng et al., 2014). This trend is in line with the increasingly younger ages of the potassic-ultrapotassic igneous rocks from north to south (Hou et al., 2003; Lu et al., 2012; Deng et al., 2014), indicating a likely genetic connection between them. Although most of these Pb-Zn deposits show little evidence of direct magmatic inputs, the fluid inclusion homogenization temperatures (~150–250 °C; Tang et al., 2011; Tao et al., 2011; Liu et al., 2016; Xu, 2017), which are higher than values expected for geological reasonable geothermal gradients and estimated stratigraphic burial temperature at the time of mineralization, are most likely explained by anomalous heat sources related to coeval magmatism. The late Eocene to early Oligocene potassic-ultrapotassic igneous activities had clear impacts on the interior of basins, as evidenced by the exposures of the Lianhuashan and Zhuopan intrusions with ages of 35–34 Ma in the Lanping Basin (Liu et al., 2017a; Du et al., 2018).

After the removal of the lithospheric mantle that generated the

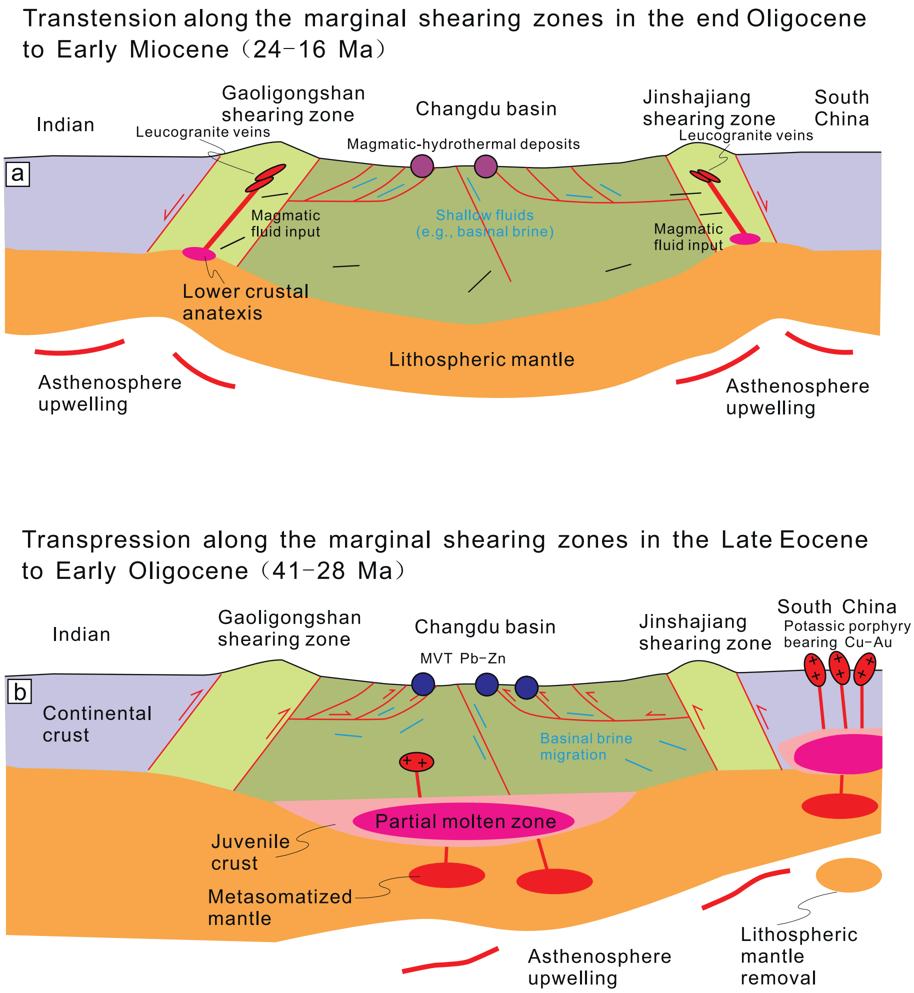

Fig. 6. Tectonic model for the formation of sediment-hosted Pb-Zn polymetallic deposits in the SMB. a During the transtensional regime, asthenospheric upwelling beneath the marginal orogens induced anatexis of lower crustal materials, resulting in leucogranite veins that contributed magmatic fluid for base metal mineralization. b During the transpressional regime associated with the removal of the lithospheric mantle under the South China block, the underplating of the asthenosphere in the basin led to partial melting of juvenile crust, which heated circulating basinal brines and drove fluid transport upwards along thrust faults to form the MVT Pb-Zn deposits (modified from Deng et al., 2014).

potassic-ultrapotassic igneous rocks, the crust of the South China block was split with a partial thrust westward underneath the Changdu - Lanping - Simao blocks, resulting in transpressional faults along the margins of those basins (Fig. 6b). In response to regional compression, voluminous basinal fluid was released and transported along the contemporaneous thrust faults, producing Pb-Zn deposits similar to MVT ore deposits elsewhere. Therefore, the base metal mineralizations of the SMB are concluded to be composed of late Eocene to early Oligocene Pb-Zn ore mineralization (e.g., Baiyangping Pb-Zn deposits) that formed in a transpressional setting and Miocene Sb(-Pb) mineralization that occurred in a transtensional setting during the India-Asia continental collision. Cenozoic Sb mineralized deposits are gradually being reported, such as the Bijiashan Sb deposits (Sb: 52664 tons; Tong et al., 2016) and the Shangnuluo and Baiji Pb-Zn-Sb deposits (Liu et al., 2021) in the Lanping Basin. Moreover, the age of Sb(-Pb) mineralization from the Baiji deposit also suggests a transtensional setting during the India-Asia continental collision (Liu et al., 2021). The similarity of the tectonic evolution between these basins in the SMB suggests that this region has significant exploration potential for Sb(-Pb) resources.

6. Conclusions

In situ U-Pb dating of calcite indicates that the Sb-Pb mineralization in the Lanuoma deposit occurred at 19.7 ± 1.6 Ma, which was likely related to contemporaneous Miocene tectono-magmatic activity in the Sanjiang Tethys region. The overprinting of the ~20 Ma Sb-Pb mineralization on early Oligocene (30 Ma) Zn mineralization during the India-Asia collision generated the characteristic Zn-Pb-Sb assemblage at Lanuoma. The discovery of Miocene Sb-Pb mineralization suggests great exploration potential for Sb(-Pb) resources within the SMB.

Declaration of competing interest

The authors declare that they have no known competing financial interests or personal relationships that could have influenced the work reported in this submission.

Acknowledgments

This research was funded by grants from the Team of the Belt and Road of the Chinese Academy of Sciences, National Natural Science Foundation of China (41973047 and 91955209), and the National Key Basic Research Program (2015CB452603). We particularly thank Dr. Roberts, N.M.W. from the Natural Environment Research Council (NERC) Isotope Geosciences Laboratory, British Geological Survey, Nottingham, UK, for providing reference material WC-1.

Appendix A. Supplementary data

Supplementary data to this article can be found online at https://doi.org/10.1016/j.gexplo.2022.107004.

References

Bi, X.W., Tang, Y.Y., Tao, Y., Wang, C.M., Xu, L.L., Qi, H.W., Lan, Q., Mu, L., 2019. Composite metallogenesis of sediment-hosted Pb-Zn-Ag-Cu base metal deposits in

the Sanjiang collisional orogen, SW China, and its deep driving mechanisms. Acta Petrol. Sin. 35, 1341–1371 (in Chinese with English abstract).
Bradley, D.C., Leach, D.L., Symons, D., Emsbo, P., Premo, W., Breit, G., Sangster, D.F., 2004. Reply to discussion on "Tectonic controls of Mississippi valley-type lead-zinc mineralization in orogenic forelands" by S.E. Kesler, J.T. Christensen, R.D. Hagni, W. Heijlen, J.R. Kyle, K.C. Misra, P. Muchez, and R. van der Voo, Mineralium Deposita. Miner. Deposita 39, 515–519.
Cao, S.Y., Liu, J.L., Leiss, B., Neubauer, F., Genser, J., 2011. Timing of initiation of left-lateral shearing along the Ailao Shan-Red River shear zone: microstructural and geochronological constraints from high temperature mylonites in Diancang Shan, SW China. In: EGU General Assembly Conference Abstracts, 11, p. 8773.
Chen, X.C., Hu, R.Z., Bi, X.W., Li, H.M., Lan, J.B., Zhao, C.H., Zhu, J.J., 2014. Cassiterite LA-MCICP-MS U/Pb and muscovite 40Ar/39Ar dating of tin deposits in the TengchongLianghe tin district, NW Yunnan, China. Miner. Deposita 49, 843–860.
Chung, S.L., Chu, M.F., Zhang, Y., Xie, Y., Lo, C.H., Lee, T.Y., Lan, C.Y., Li, X., Zhang, Q., Wang, Y., 2005. Tibetan tectonic evolution inferred from spatial and temporal variations in post-collisional magmatism. Earth-Sci. Rev. 68, 173–196.
Deng, J., Wang, Q.F., Li, G.J., Santosh, M., 2014. Cenozoic tectono-magmatic and metallogenic processes in the Sanjiang region, southwestern China. Earth Sci. Rev. 138, 268–289.
Du, B., Wang, C.M., Yang, L.F., Shi, K.X., Zhang, D., Chen, Q., Zhu, J.X., Zhang, S.H., 2018. Magma source and formation mechanism of the Zhuopan alkaline complex in Yongping, Southwest China: constraints from geochemistry, zircon U-Pb geochronology and Hf isotopes. Acta Petrol.Sin. 34, 1376–1396 (in Chinese with English abstract).
Feng, D.X., Hu, X.C., Xiao, F.Q., Song, X.L., Xiao, S.B., 2006. Report of Evaluation on the Lanuoma Pb-Zn Polymetallic Deposit in Changdu Area, Tibet. Geological Survey Institute of Tibet Autonomous Region.
Feng, C.X., Liu, S., Bi, X.W., Hu, R.Z., Chi, G.X., Chen, J.J., Feng, Q., Guo, X.L., 2017. An investigation of metallogenic chronology of eastern ore block in Baiyangping Pb-Zn-Cu-Ag polylmetallic ore deposit, Lanping Basin, western Yunnan Province. Miner. Depos. 36, 691–704 (in Chinese with English abstract.
Flower, M.F.J., Hoàng, N., Lo, C.H., Chí, C.T., Cu'ò'ng, N.Q., Liu, F.T., Deng, J.F., Mo, X. X., 2013. Potassic magma genesis and the Ailao Shan-Red River Fault. J. Geodyn. 69, 84–105.
Guo, L.G., Liu, Y.P., Xu, W., Zhang, X.C., Qin, K.Z., Li, T.S., Shi, Y.R., 2006. Constraints to the mineralisation age of the Yulong porphyry copper deposit from SHRIMP U-Pb zircon data in Tibet. Acta Petrol. Sin. 21, 1009–1016 (in Chinese with English abstract).
He, L.Q., Song, Y.C., Chen, K.X., Hou, Z.Q., Yu, F.M., Yang, Z.S., Wei, J.Q., Li, Z., Liu, Y. C., 2009. Thrust-controlled, sediment-hosted, Himalayan Zn-Pb-Cu-Ag deposits in the Lanping foreland fold belt, eastern margin of Tibetan Plateau. Ore Geol. Rev. 36, 106–132.
Hou, Z.Q., Cook, N.J., 2009. Metallogenesis of the Tibetan collisional orogen: a review and introduction to the special issue. Ore Geol. Rev. 36, 2–24.
Hou, Z.Q., Zhang, H.R., 2015. Geodynamics and metallogeny of the eastern Tethyan metallogenic domain. Ore Geol. Rev. 70, 346–384.
Hou, Z.Q., Ma, H.W., Khin, Z., Zhang, Y.Q., Wang, M.J., Wang, Z., Pan, G.T., Tang, R.L., 2003. The Himalayan Yulong porphyry copper belt: product of large-scale strike-slip faulting in eastern Tibet. Econ. Geol. 98, 125–145.
Hou, Z.Q., Pan, G.T., Wang, A.J., Mo, X.X., Tian, S.H., Sun, X.M., Ding, L., Wang, E.Q., Gao, Y.F., Xie, Y.L., Zeng, P.S., Qin, K.Z., Xu, J.F., Qu, X.M., Yang, Z.M., Yang, Z.S., Fei, H.C., Meng, X.J., Li, Z.Q., 2006. Metallogenesis in Tibetan collisional orogenic belt: II. Mineralization in late-collisional transformation setting. Miner.Depos. 25, 521–543 (in Chinese with English abstract).
Hou, Z.Q., Song, Y.C., Li, Z., Wang, Z.L., Yang, Z.M., Yang, Z.S., Liu, Y.C., Tian, S.H., He, L.Q., Chen, K.X., Wang, F.C., Zhao, C.X., Xue, W.Z., Lu, H.F., 2008. Thrust-controlled, sediment-hosted Pb-Zn-Ag-Cu deposits in eastern and northern margins of Tibetan orogenic belt: geological features and tectonic model. Miner.Depos. 27, 123–144 (in Chinese with English abstract).
Hu, Z.C., Gao, S., Liu, Y.S., Hu, S.H., Chen, H.H., Yuan, H.L., 2008. Signal enhancement in laser ablation ICP-MS by addition of nitrogen in the central channel gas. J. Anal. At. Spectrom. 23, 1093–1101.
Janković, S., Mozgova, N.N., Borodaev, Y.S., 1977. The complex antimony-lead/zinc deposit at Rujevac/Yugoslavia; its specific geochemical and mineralogical features. Miner. Deposita 12, 381–392.
Jiang, Y.H., Jiang, S.Y., Ling, H.F., Dai, B.Z., 2006. Low-degree melting of a metasomatized lithospheric mantle for the origin of Cenozoic Yulong monzogranite-porphyry, east Tibet: geochemical and Sr-Nd-Pb-Hf isotopic constraints. Earth Planet. Sci. Lett. 241, 617–633.
Kesler, S.E., Chesley, J.T., Christensen, J.N., Hagni, R.D., Heijlen, W., Kyle, J.R., Muchez, P., Misra, K.C., van der Voo, R., 2004. Discussion of "Tectonic controls of Mississippi Valley-type lead-zinc mineralization in orogenic forelands" by D.C. Bradley and D.L.Leach. Miner. Deposita 39, 512–514.
Leach, D.L., Song, Y.C., 2019. Sediment-hosted zinc-lead and copper deposits in China. In: Economic Geology SEG Special Publication, pp. 1–86.
Leach, D.L., Song, Y.C., Hou, Z.Q., 2017. The world-class Jinding Zn-Pb deposit: ore formation in an evaporite dome, Lanping Basin, Yunnan, China. Miner. Deposita 52, 281–296.
Liao, Z.T., Chen, Y.K., 2005. Nature and evolution of Lanping-Simao basin prototype. J. Tongji Univ. 33, 1528–1531 (in Chinese with English abstract).
Liu, J.L., Song, Z.J., Cao, S.Y., Zhai, Y.F., Wang, A.J., Gao, L., Xiu, Q.Y., Cao, D.H., 2006. The dynamic setting and processes of tectonic and magmatic evolution of the oblique collision zone between Indian and Eurasian plates: exemplified by the tectonic evolution of the Three River region, eastern Tibet. Acta Petrol. Sin. 4, 755–786 (in Chinese with English abstract).
Liu, Y.S., Hu, Z.C., Gao, S., Günther, D., Xu, J., Gao, C.G., Chen, H.H., 2008. In situ analysis of major and trace elements of anhydrous minerals by LA-ICP-MS without applying an internal standard. Chem. Geol. 257, 34–43.
Liu, J.L., Tang, Y., Tran, M.D., Cao, S.Y., Zhao, L., Zhang, Z.C., Zhao, Z.D., Chen, W., 2012. The nature of the Ailao Shan-Red River (ASRR) shear zone: constraints from structural, microstructural and fabric analyses of metamorphic rocks from the Diancang Shan, Ailao Shan and Day Nui Con Voi massifs. J. Asian Earth Sci. 47, 231–251.
Liu, F.L., Wang, F., Liu, P.H., Yang, H., Meng, E., 2015. Multiple partial melting events in the Ailao Shan-Red River and Gaoligong Shan complex belts, SE Tibetan Plateau: zircon U-Pb dating of granitic leucosomes within migmatites. J. Asian Earth Sci. 110, 151–169.
Liu, Y.C., Hou, Z.Q., Yang, Z.S., Tian, S.H., Song, Y.C., Yu, Y.S., Ma, W., 2016. Geology and chronology of the Zhaofayong carbonate-hosted Pb-Zn ore cluster: implication for regional Pb–Zn metallogenesis in the Sanjiang belt,Tibet. Gondwana Res. 35, 15–26.
Liu, J.Y., Deng, J., Li, G.J., Xiao, C.H., Meng, F.J., Chen, F.C., Wu, W., Zhang, Q.W., 2017a. Petrogenesis and tectonic significance of the Lianhuashan intrusion in the Lanping Basin, western Yunnan: constraints from bulk element composition, zircon U-Pb geochronology and Hf isotopic compositions. Acta Petrol. Sin. 33, 2115–2128 (in Chinese with English abstract).
Liu, Y.C., Kendrick, M.A., Hou, Z.Q., Yang, Z.S., Tian, S.H., Song, Y.C., Honda, M., 2017b. Hydrothermal fluid origins of carbonate-hosted Pb-Zn deposits of the Sanjiang Thrust Belt, Tibet: indications from noble gases and halogens. Econ. Geol. 112, 1247.
Liu, Y.F., Qi, H.W., Bi, X.W., Hu, R.Z., Qi, L.K., Yin, R.S., Tang, Y.Y., 2021. Two types of sediment-hosted Pb-Zn deposits in the northern margin of Lanping basin, SW China: evidence from sphalerite trace elements, carbonate C-O isotopes and molybdenite Re-Os age. Ore Geol. Rev. 131 https://doi.org/10.1016/j.oregeorev.2021.104016.
Lu, Y.J., Kerrich, R., Cawood, P.A., McCuaig, T.C., Hart, C.J.R., Li, Z.X., Hou, Z.Q., Bagas, L., 2012. Zircon SHRIMP U-Pb geochronology of potassic felsic intrusions in western Yunnan, SW China: constraints on the relationship of magmatism to the Jinsha suture. Gondwana Res. 22, 737–747.
Metcalfe, I., 2002. Permian tectonic framework and palaeogeography of SE Asia. J. Asian Earth Sci. 20, 551–566.
Mu, C.L., Wang, J., Yu, Q., Zhang, L.S., 1999. The evolution of the sedimentary basin in Lanping area during Mesozoic-Cenozoic. J.Mineral.Petrol. 19, 30–36 (in Chinese with English abstract).
Mu, L., Hu, R.Z., Bi, X.W., Tang, Y.Y., Lan, T.G., Lan, Q., Zhu, J.J., Peng, J.T., Oyebamiji, A., 2021. New insights into the origin of the world-class Jinding sediment-hosted Zn-Pb deposit, southwestern China: evidence from LA-ICPMS analysis of Individual fluid inclusions. Econ. Geol. https://doi.org/10.5382/econgeo.4826.
Pan, G.T., Chen, Z.L., Li, X.Z., 1997. Tectonic Evolution of the East Tethys Geology. Geological Publishing House, Beijing.
Pan, G.T., Xu, Q., Hou, Z.Q., Wang, L.Q., Du, D.X., Mo, X.X., Li, D.M., Wang, M.J., Jiang, X.S., Hu, Y.Z., 2003. The Ore-forming System of the Orogenic Processing in the Western "Sanjiang" Poly-arc And the Resources Estimate. Geological Publishing House, Beijing.
Pan, G.T., Ding, J., Yao, D.S., Wang, L.Q., 2004. Geological Map of Qinghai-Xizan (Tibet) Plateau And Adjacent Area. Chengdu Cartographic Press, Chengdu (in Chinese).
Radosavljević, S.A., Stojanović, J.N., Radosavljević-Mihajlović, A.S., Vuković, N.S., 2014. Rujevac Sb-Pb-Zn-As polymetallic deposit, Boranja orefield, Western Serbia: native arsenic and arsenic mineralisation. Mineral. Petrol. 108, 111–122.
Radosavljević, S.A., Stojanović, J.N., Radosavljević-Mihajlović, A.S., Vuković, N.S., 2016. (Pb-Sb)-bearing sphalerite from the Čumavići polymetallic ore deposit, Podrinje Metallogenic District, East Bosnia and Herzegovina. Ore Geol. Rev. 72, 253–268.
Roberts, N.M.W., Walker, R.J., 2016. U-Pb geochronology of calcite-mineralized faults: absolute timing of rift-related fault events on the northeast Atlantic margin. Geology 44, 531–534.
Roberts, N.M.W., Rasbury, E.T., Parrish, R.R., Smith, C.J., Horstwood, M.S.A., Condon, D.J., 2017. A calcite reference material for LA-ICP-MS U-Pb geochronology. Geochem.Geophys.Geosyst. 18, 2807–2814.
Searle, M.P., Yeh, M.W., Lin, T.H., Chung, S.L., 2010. Structural constraints on the timing of left-lateral shear along the Red River shear zone in the Ailao Shan and Diancang Shan Ranges, Yunnan, SW China. Geosphere 6, 316–338.
Sheng, X.Y., Bi, X.W., Hu, R.Z., Tang, Y.Y., Lan, Q., Xiao, J.F., Tao, Y., Huang, M.L., Peng, J.T., Xu, L.L., 2019. The mineralisation process of the Lanuoma Pb-Zn-Sb deposit in the Sanjiang Tethys region: Constraints from in situ sulfur isotopes and trace element compositions. Ore Geol. Rev. 111 https://doi.org/10.1016/j.oregeorev.2019.102941.
Song, Y.C., Hou, Z.Q., Liu, Y.C., Zhang, H.R., 2017. Mississippi Valley-Type (MVT) Pb- Zn deposits in the Tethyan domain: a review. Geol. China 44, 664–689 (in Chinese with English abstract).
Spurlin, M.S., Yin, A., Horton, B.K., Zhou, J.Y., Wang, J.H., 2005. Structural evolution of the Yushu-Nangqian region and its relationship to syncollisional igneous activity, eastcentral Tibet. Geol. Soc. Am. Bull. 117, 1293–1317.
Tang, J.X., Zhong, K.H., Liu, Z.C., Li, Z.J., Dong, S.Y., Zhang, L., 2006. Intracontinent orogeny and metallogenesis in Himalayan epoch: Changdu large composite basin, eastern Tibet. Acta Petrol. Sin. 80, 1364–1376 (in Chinese with English abstract).
Tang, Y.Y., Bi, X.W., He, L.P., Wu, L.Y., Feng, C.X., Zou, Z.C., Tao, Y., Hu, R.Z., 2011. Geochemical characteristics of trace elements, fluid inclusions and carbon-oxygen isotopes of calcites in the Jinding Zn-Pb deposit, Lanping, China. Acta Petrol. Sin. 27, 2635–2645 (in Chinese with English abstract).
Tang, Y., Liu, J.L., Tran, M.D., Song, Z.J., Wu, W.B., Zhang, Z.C., Zhao, Z.D., Chen, W., 2013. Timing of left-lateral shearing along the Ailao Shan-Red River shear zone:

constraints from zircon U-Pb ages from granitic rocks in the shear zone along the Ailao Shan Range, Western Yunnan, China. Int. J. Earth Sci. 102, 605–626.
Tang, Y.Y., Bi, X.W., Fayek, M., Stuart, F.M., Wu, L.Y., Jiang, G.H., Xu, L.L., Liang, F., 2017. Genesis of the Jinding Zn-Pb deposit, northwest Yunnan Province, China: constraints from rare earth elements and noble gas isotopes. Ore Geol. Rev. 90, 970–986.
Tao, Y., Bi, X.W., Xin, Z.L., Zhu, F.L., Liao, M.Y., Li, Y.B., 2011. Geology, geochemistry and origin of Lanuoma Pb-Zn-Sb deposit in Changdu area,Tibet. Miner. Depos. 30, 599–615 (in Chinese with English abstract).
Tao, Y., Bi, X.W., Li, C.S., Hu, R.Z., Li, Y.B., Liao, M.Y., 2014. Geochronology, petrogenesis and tectonic significance of the Jitang granitic pluton in eastern Tibet, SW China. Lithos 184, 214–323.
Tapponnier, P., Lacassin, R., Leloup, P.H., 1990. The Ailao Shan-Red River metamorphic belt, Tertiary left lateral shear between Indochina and South China. Nature 343, 431–437.
Taylor, B.E., 1986. Magmatic volatiles: isotope variation of C, H and S reviews in mineralogy. In: Stable Isotopes in High Temperature Geological Process, 16. Mineralogical Society of America, pp. 185–226.
Tong, Z.D., Zhang, J., Li, T.J., 2016. Geology and fluid inclusion of the Bijiashan Sb deposit in western Yunnan Province. Acta Petrol. Sin. 32, 2379–2391 (in Chinese with English abstract).
Veizer, J., Holser, W.T., Wilgus, C.K., 1980. Correlation of 13C12C and 34S32S secular variations. Geochim. Cosmochim. Acta 44, 579–587.
Wang, G.Z., Liu, D.Z., Zhu, L.D., Tao, X.F., Li, Y.G., 2000. Analysis of the undating metamorphics in West Yunnan and determination of its age. Reg.Geol.China 19, 32–37 (in Chinese with English abstract).
Wang, J.H., Yin, A., Harrison, T.M., Grove, M., Zhang, Y.Q., Xie, G.H., 2001. A tectonic model for Cenozoic igneous activities in the eastern Indo-Asian collision zone. Earth Planet. Sci. Lett. 188, 123–133.
Wang, Y.J., Fan, W.M., Zhang, Y.H., Peng, T.P., Chen, X.Y., Xu, Y.G., 2006. Kinematics and 40Ar/39Ar geochronology of the Gaoligong and Chongshan shear systems, western Yunnan, China: implications for Early Oligocene tectonic extrusion of SE Asia. Tectonophysics 418, 235–254.
Wang, Q., Wyman, D.A., Li, Z.X., Sun, W.D., Chung, S.L., Vasconcelos, P.M., Zhang, Q.Y., Dong, H., Yu, Y.S., Pearson, N., Qiu, H.N., Zhu, T.X., Feng, X.T., 2010. Eocene north-south trending dikes in central Tibet: new constraints on the timing of eastwest extension with implications for early plateau uplift? Earth Planet. Sci. Lett. 298, 205–216.
Wang, X.H., Hou, Z.Q., Song, Y.C., Yang, T.N., Zhang, H.R., 2011a. Baiyangping Pb-Zn-Ag-Cu polymetallic deposit in Lanping basin: metallogenic chronology and regional mineralization. Acta Petrol. Sin. 27, 2625–2634 (in Chinese with English abstract).
Wang, X.H., Song, Y.C., Hou, Z.Q., Zhang, H.R., Liu, Y.C., Yang, Z.S., Yang, T.N., Pan, X. F., Wang, S.X., Xue, C.D., 2011b. Characteristics of trace elements and S-Pb isotopes in sphalerites from lead-zinc polymetallic deposits in Fulongchang area, Lanping Basin, western Yunnan Province, and their implications. Acta Petrol. Mineral. 30, 45–59 (in Chinese with English abstract).
Wang, C.M., Chen, J.Y., Yang, L.F., Zhang, D., Du, B., Shi, K.X., 2017. Tectonic-fluid-mineral system in the Lanping basin, Sanjiang Tethys. Acta Petrol. Sin. 33, 1957–1977 (in Chinese with English abstract).
Wang, D., Zheng, Y.Y., Mathur, R., Jiang, J.S., Zhang, S.K., Zhang, J.F., Yu, M., 2019. Multiple mineralisation events in the Zhaxikang Sb–Pb–Zn–Ag deposit and their relationship with the geodynamic evolution in the North Himalayan Metallogenic Belt, South Tibet. Ore Geol. Rev. 105, 201–215.
Xie, Y.L., Li, L.M., Wang, B.G., Li, G.M., Liu, H.F., Li, Y.X., Dong, S.L., Zhou, J.J., 2017. Genesis of the Zhaxikang epithermal Pb-Zn-Sb deposit in southern Tibet, China: evidence for a magmatic link. Ore Geol. Rev. 80, 891–909.
Xu, C.X., 2017. In: Geochemical Features And Ore Genesis of Sediment-hosted Lead-zinc Deposits in the Changdu Area, Tibet— Exemplified by Lanuoma And Cuona Pb-Zn Deposits. University of Chinese Academy of Sciences, Guiyang, pp. 1–140 (in Chinese with English abstract).
Xu, Y.G., Lan, J.B., Yang, Q.J., Huang, X.L., Qiu, H.N., 2008. Eocene break-off of the NeoTethyan slab as inferred from intraplate-type mafic dykes in the Gaoligong orogenic belt, eastern Tibet. Chem. Geol. 255, 439–453.
Xu, Y.G., Yang, Q.J., Lan, J.B., Luo, Z.Y., Huang, X.L., Shi, Y.R., Xie, L.W., 2012. Temporal–spatial distribution and tectonic implications of the batholiths in the Gaoligong-Tengliang-Yingjiang area, western Yunnan: constraints from zircon U-Pb ages and Hf isotopes. J. Afr. Earth Sci. 53, 151–175.
Yalikun, Y.X.E., Xue, C.J., Symons, D.T.A., 2018. Paleomagnetic age and tectonic constraints on the genesis of the giant Jinding Zn-Pb deposit, Yunnan, China. Miner. Deposita 53, 245–259.
Yang, C., 2011. Researches on Ore-forming Materials And Ore-forming Fluid's Sources in the Lanuoma Pb-Zb Polymetallic Deposit, Eastern Tibet. Institute of Geochemistry, Chinese Academy of Sciences.
Yin, A., Harrison, T.M., 2000. Geologic evolution of the Himalayan-Tibetan orogen. Annu. Rev. Earth Planet. Sci. 28, 211–280.
Yin, H.F., Wu, S.B., Du, Y.S., Peng, Y.Q., 1999. South China defined as part of Tethyan archipelagic ocean system. Earth Sci.J.China Univ.Geosci. 24, 1–12 (in Chinese with English abstract).
Zhai, M.G., Cong, B.L., 1993. The diancangshan-Shigu metamorphic belt in W. Yunnan, China: their geochemical and geochronological characteristics and division of metamorphic domains. Acta Petrol. Sin. 9, 227–239 (in Chinese with English abstract).
Zhang, B., Zhang, J.J., Zhong, D.L., 2010. Structure, kinematics and ages of transpression during strain-partitioning in the Chongshan shear zone, western Yunnan, China. J. Struct. Geol. 32, 445–463.
Zhang, H.S., Ji, W.H., Yang, X.Y., Zhou, J.X., Sun, C., Jia, Z.Y., Hong, J., Lv, P.R., Zhao, Z., Hou, Q., 2019. The origin of the Quemocuo carbonate-hosted Pb-Zn deposit in the Sanjiang Tethyan Belt, SW China: constrained by Sm-Nd isochronic age and Sr-S-Pb isotope compositions. Ore Geol. Rev. 117 https://doi.org/10.1016/j.oregeorev.2019.103264.
Zhong, D.L., 1998. Paleo-Tethyan Orogenic Belt in Western Yunnan And Sichuan. Science Press, Beijing.
Zhong, D.L., Ding, L., Liu, F.T., Liu, J.H., Zhang, J.J., Ji, J.Q., Chen, H., 2000. Poly-layered architecture of lithosphere in orogen and its constraint on Cenozoic magmatismexample from Sanjiang and surrounding area. Sci.China (Ser.D) 30 (S1), 1–8 (in Chinese).
Zhou, M.F., Robinson, P.T., Wang, C.Y., Zhao, J.H., Yan, D.P., Gao, J.F., Malpas, J., 2012. Heterogeneous mantle source and magma differentiation of quaternary arc-like volcanic rocks from Tengchong, SE margin of the Tibetan Plateau. Contrib. Mineral. Petrol. 163, 841–860.
Zhou, Q., Li, W.C., Qing, C.S., Lai, Y., Li, Y.X., Liao, Z.W., Wu, J.Y., Wang, S.W., Dong, L., Tian, E.Y., 2018. Origin and tectonic implications of the Zhaxikang Pb-Zn-Sb-Ag deposit in northern Himalaya: evidence from structures, Re-Os-Pb-S isotopes, and fluid inclusions. Miner.Deposita 53, 585–600.
Zou, Z.C., Hu, R.Z., Bi, X.W., Wu, L.Y., Feng, C.X., Tang, Y.Y., 2015. Absolute and relative dating of Cu and Pb-Zn mineralization in the Baiyangping area, Yunnan Province, SW China: Sm-Nd geochronology of calcite. Geochem. J. 49, 103–112.